

UNIVERSITY OF OTTAWA

MCG4322

RE3 - WILDCAT ENGINEERING

Capstone Report

Volume x of y

Joey Kane - 7386330

Isaak Goldenberg - 7395188

Sawyer Woodside - 7158568

Alex Pennell - 7334789

December 8, 2017



Sponsor: Dr. Eric Lanteigne

Abstract

- i. Contents of each book (if applicable)
 - ii. Description of design
 - iii. Special considerations
 - iv. Illustration of the final design
- half page, one paragraph

Contents

1	Introduction	1
1.1	Project Mandate	1
1.2	Group Problem Scope	1
1.3	Criteria and Restrictions	1
1.4	Parameterization Overview	1
2	Proposed Design	5
3	Analysis	7
3.1	Thruster Arm Adhesion	7
A	Instructions for Installing and Running the GUI	11
B	Code	13
B.1	Code 1	13
C	Additional Material	19
C.1	Thrust Force	19
C.2	Cauchy Stress Tensor [25]	26
D	Data Sheets	27
D.1	Linear Actuator [1]	27
D.2	Bearings [16]	28
D.3	Friction Wheel Assembly	29
D.3.1	Friction Wheel [15]	29
D.3.2	Friction Wheel Set Screw [17]	30
D.3.3	Friction Wheel Motor [20]	31
D.3.4	Friction Wheel Encoder [21]	32
D.4	Spring [18]	33
D.5	Battery [5]	34
D.6	Thruster Assembly	35
D.6.1	Thruster Motor [12]	35
D.6.2	Propeller [10]	36
D.6.3	BESC [6]	37
D.6.4	Servo Motor [22]	38
D.6.5	Receiver [11]	40

D.7 Flight Control Assembly	41
D.7.1 ESC [7]	41
D.7.2 GPS Module [9]	42
D.7.3 Transceiver [13]	43
D.7.4 Flight Controller [8]	44
E Engineering Drawings	45
E.1 Parts List	45
E.2 Complete System Drawing	45
E.3 Sub-Assembly Drawings	45
E.4 Individual Part Drawings	45
F Meeting Minutes	47
G Recommendations for Improving the Course	49

List of Figures

1.1	Overview of Modelling Paramaterization	2
1.2	Detailed Modelling Paramaterization	3
3.1	Analysis of Carbon Fibre Adhesion (From Shigley's Machine Design [3, 484])	7
C.1	Graph of Thrust Plotted Against Airship Speed at 11000rpm With 7", 5" Pitch Diameter Propeller	22
C.2	Test Data from Gabriel Staples Against Experimental Static Thrust Values [24]	23
C.3	Test Data from Gabriel Staples Against Experimental Dynamic Thrust Values [24]	24
C.4	Sample Thrust Calculation Using On-line Calculator [4]	25

List of Tables

C.1 Table of Calculated Thrust Values for Varying Airship Speeds	21
--	----

Nomenclature

E_p	Modulus of elasticity of considered plastic hub or boss [N/mm^2]
F_R	Keel to assembly arm connector reaction, [N]
F_T	Thruster force, [N]
F_g	Force of gravity, [N]
F_{GR}	Reaction force of gondola, [N]
F_{K1}	Keel reaction force 1, [N]
F_{K2}	Keel reaction force 2, [N]
F_{LA}	Linear actuator force, [N]
F_{NB}	Normal force applied to bearing, [N]
F_{RSF}	Force of snap fit bearing [N]
F_α	Force on fastener α (hinge to gondola), [N]
F_β	Force on fastener β (hinge to gondola), [N]
F_a	Force on fastener a (hinge to gondola), [N]
F_{bolt}	Bolt pretension force, [N]
F_{brake}	Normal braking force keel reaction, [N]
F_b	Force on fastener b (hinge to gondola), [N]
F_{c1}	Connector moment couple force 1, [N]
F_{c2}	Connector moment couple force 2, [N]
F_{ffric}	Friction force acting on friction wheel, [N]
F_{nfric}	Normal force acting on friction wheel, [N]
F_{s1}	Force on friction wheel motor fastener 1 , [N]
F_{s2}	Force on friction wheel motor fastener 2 , [N]
F_{spring}	Force applied by hinge spring, [N]
H_{keel}	Height of the bearing arm contact point on the keel, [m]

L_G	Width of gondola, [m]
L_a	Length from pivot point of hinge to fastener a , [m]
L_b	Length from pivot point of hinge to fastener b , [m]
L_m	Length from side of gondola to gondola drive motor hinge, [m]
L_s	Length from fastener to fastener of gondola motor to hinge, [m]
L_{SF}	Length to snap fit bearing, [m]
L_{ac}	Length from centerline of gondola to fastener a, [m]
L_{bc}	Length from centerline of gondola to fastener b, [m]
L_{cm}	Length from gondola wall to center of mass of gondola, [m]
$L_{contact}$	Length from contact to contact of bearings on keel, [m]
L_{drive}	Length of gondola hinge to friction wheel contact, [m]
L_{hs}	Distance from the pivot of the hinge to the gondola motor fastener, [m]
L_{hw}	Distance from the gondola motor fastener to the contact point of the friction wheel, [m]
L_{rx}	Friction wheel motors shaft length, [m]
M_1	Reaction moment on bearing arm, [Nm]
M_R	Connector moment reaction, [Nm]
R	Reaction force, [N]
$S_{compressive}$	Compressive strength of gondola material, [Pa]
T_w	Friction wheel motor torque, [Nm]
T_{spring}	Torque of hinge spring, [Nm]
W_A	Weight of thruster assembly arm, [N]
W_E	Weight of thruster enclosure, [N]
W_T	Weight of thruster, [N]
W_c	Weight of connection piece, [N]
W_{LA}	Weight of linear actuator, [N]

η	Safety Factor
μ	Coefficient of friction
σ'	Von Mises Stress, [Pa]
σ_{washer}	Compressive force of washer, [Pa]
σ_x	Principle stress, [Pa]
σ_a	Hoop stress, [N/mm ²]
σ_s	Allowable design stress for plastic, N/mm ²
$a_{airship}$	Acceleration of airship, [m/s]
$a_{gondola1}$	Acceleration of Gondola 1 , [m/s ²]
$a_{gondola2}$	Acceleration of Gondola 2 , [m/s ²]
c	Distance from neutral axis to stress location, [m]
d_i	Interference diameter, [mm]
d_s	Hub outer diameter, [mm]
d_s	Shaft diameter, [mm]
i_a	Allowable interference, [mm]
$m_{airship}$	Mass of airship, [kg]
$m_{gondola1}$	Mass of Gondola 1, [kg]
$m_{gondola2}$	Mass of Gondola 2, [kg]
r_{fw}	Radius of friction wheel, [m]
w_{armx}	Width of the bearing arm in the x direction, [m]
w_{army}	Width of the bearing arm in the y direction, [m]

Chapter 1: Introduction

1.1 Project Mandate

The goal of the project is to overcome the current limitations involved with the control and landing of unmanned airships in adverse outdoor conditions. The airship consists of a helium filled envelope, external keel, and gondola which will act as a ballast. The moving ballast will control the pitch by the controlled displacement of the centre of mass. Propulsion will be provided by propellers in the X-Y plane of the airship. The system will have vector thrusting to allow for altitude change independent of pitch change.

1.2 Group Problem Scope

The research project led by Dr. Eric Lanteigne involves designing a system to allow for the control of an unmanned airship. The goal of the project is to create a system that controls the airship by changing the position of the centre of mass to initiate pitch change. This pitch change, along with forward propulsion, will drive the airship in a given direction. The design team will be responsible for creating a system, where a gondola that acts as a ballast, will move along a nonlinear, diamond-shaped keel in order to initiate pitch change of an airship. Ideally, the system will be able to incur a pitch change of up to ninety degrees, allowing the airship to descend straight downwards. Currently, all designs must be scalable as specifications of the airship envelope have yet to be finalized. The unmanned airship must be capable of flying outdoors and be able to carry a payload of between 0.2kg and 0.5kg. The main components of the design can be split up into: Gondola Design, Gondola Movement, Securing Gondola to Keel, Gondola Position Measurement, Securing the Propellers, Thrust Vectoring, Batteries, and Wire Management.

1.3 Criteria and Restrictions

The propellers will be in the X-Y plane, in line with the centre of volume. This eliminates any moments from the propellers that lead to imbalance and unwanted pitch variations. The gondola will be able to move along the varying curvature of the keel using a hinged-gondola. The driving mechanism will be two friction wheels with the additional support of 4 driven bearings. The cross-section of the keel is diamond-shaped, however it is not torsionally constant, therefore the vertexes are not coincident on the curved section. Once the airship has been constructed, a Special Flight Operations Certificate (SFOC) issued by Transport Canada will be necessary in order to fly the airship lawfully.

1.4 Parameterization Overview

A high level overview of the system's parameterization is shown in Figure 1.1.

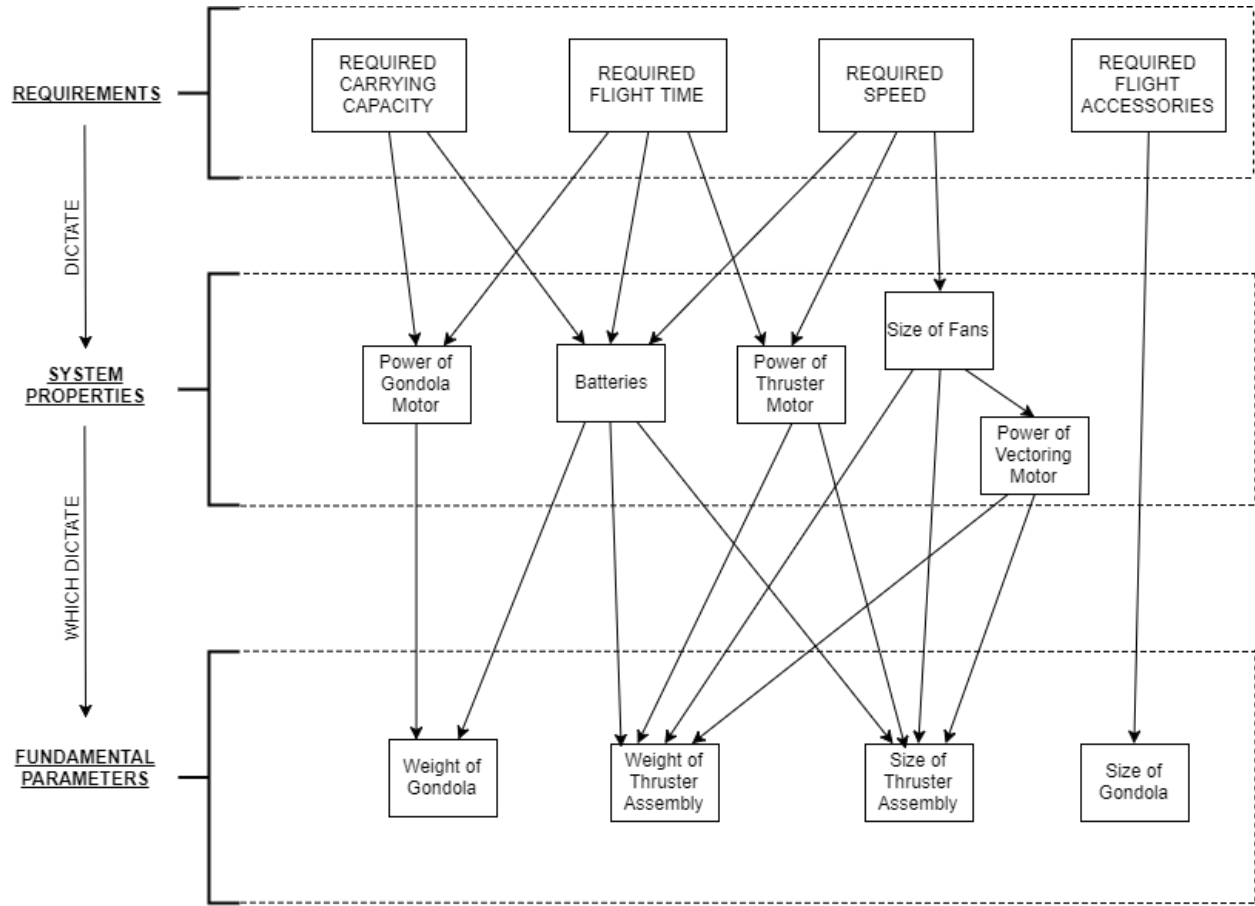


Figure 1.1: Overview of Modelling Parameterization

Figure 1.2 is a more detailed parameterization outline, which shows how user inputs will be converted to forces using an iterative approach. This approach will be used to compute all forces shown in Section ADD HERE.

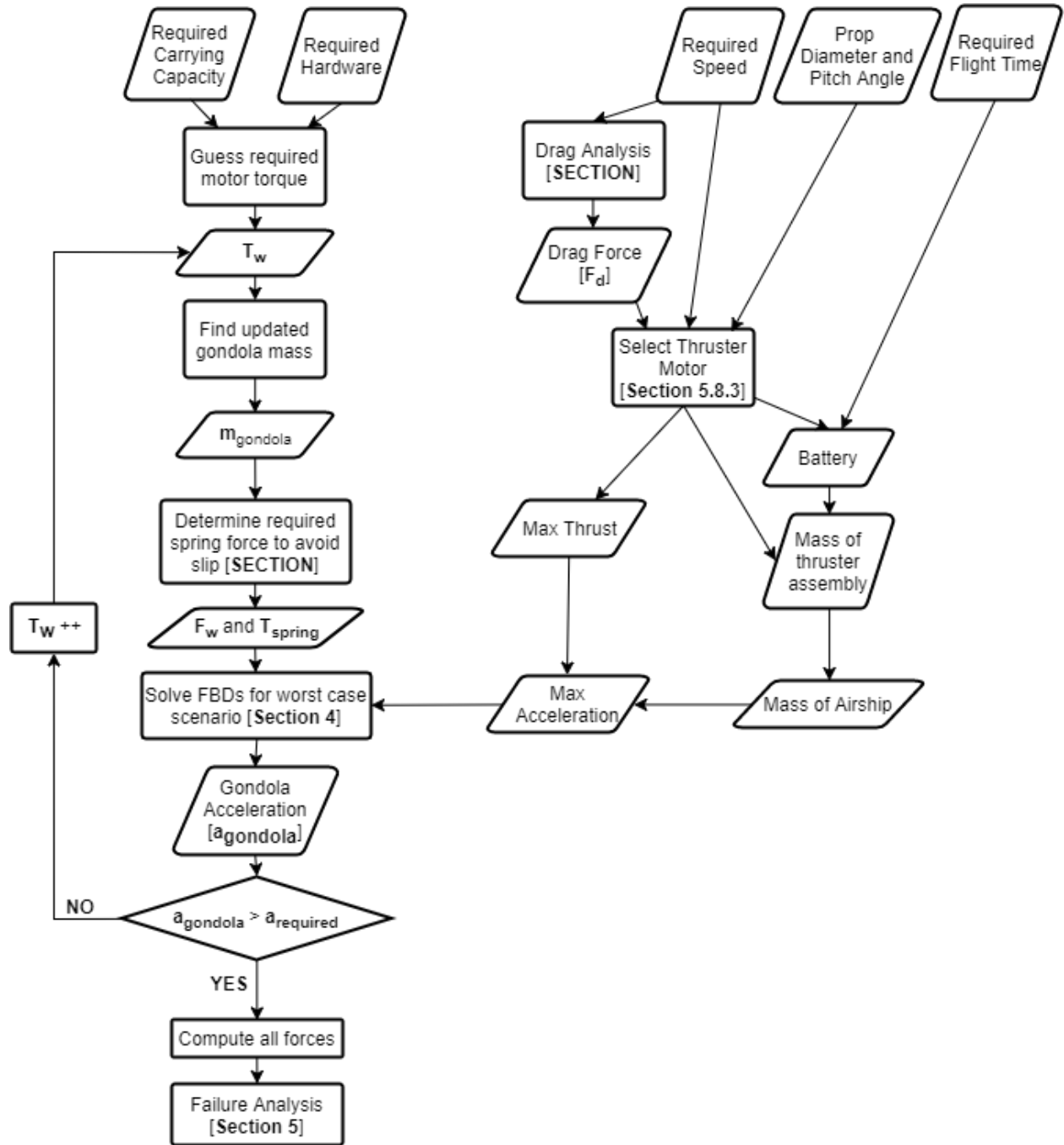


Figure 1.2: Detailed Modelling Parameterization

Once all of the forces acting on the body are computed, failure analyses for each part are conducted in Section ADD HERE.

Chapter 2: Proposed Design

Text

Chapter 3: Analysis

3.1 Thruster Arm Adhesion

To connect the carbon fibre arm to the aluminium body which holds the thruster assembly, epoxy will be used. The carbon fibre arm will slide into an aluminium pocket welded to the aluminium thruster plate, as shown in Figure **ADD RENDERED FIGURE HERE**.

The analysis will be conducted by assuming the adhesion surface will be like a double lap joint, shown in Figure 3.1 below.

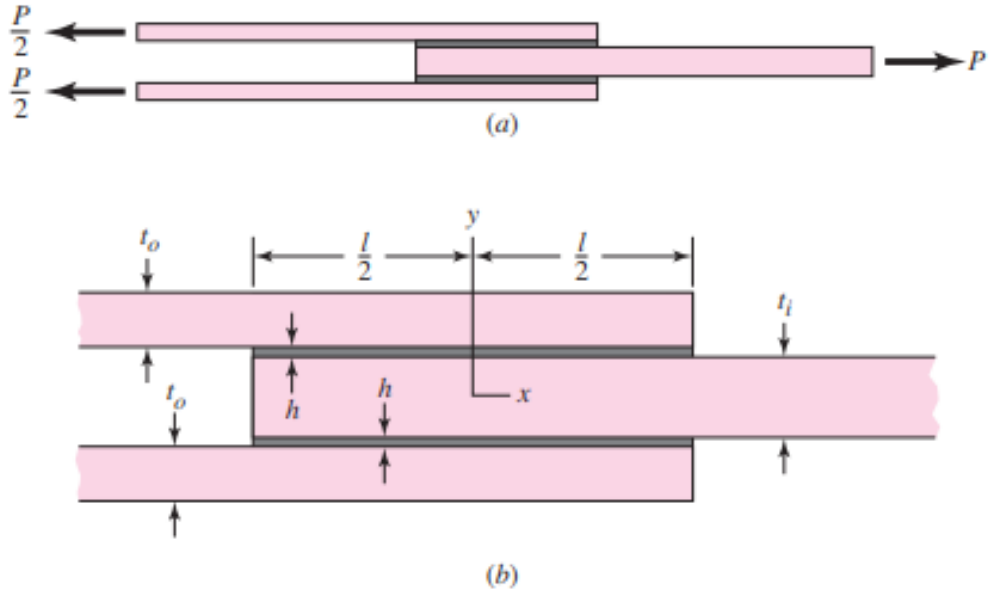


Figure 3.1: Analysis of Carbon Fibre Adhesion (From Shigley's Machine Design [3, 484])

The shear-stress distribution of the joint is given by

$$\tau(x) = \frac{P\omega}{4bsinh(\omega l/2)}cosh(\omega x) + \left[\frac{P\omega}{4bcosh(\omega l/2)} \left(\frac{2E_0t_0 - E_it_i}{2E_0t_0 + E_it_i} \right) + \frac{(\alpha_i - \alpha_0)\Delta T\omega}{(1/E_0t_0 + 2/E_it_i)cosh(\omega l/2)} \right] sinh(\omega x) \quad (3.1)$$

$$\omega = \sqrt{\frac{G}{h} \left(\frac{1}{E_0t_0} + \frac{2}{E_it_i} \right)} \quad (3.2)$$

Where E_o , t_0 α_0 and E_i , t_i α_i are the modulus, thickness, coefficient of thermal expansion for the outer and inner adherend, respectively. G , h , b and l are the shear modulus, thickness, width and length of the adhesive, respectively. ΔT is the change in temperature of the joint, from its curing temperature (zero

stress temperature). The closer the curing temperature of the adhesive is to the operating temperature, the lower the thermal stresses induced in the joint will be.

For this case, an unmodified epoxy will be selected as the adhesive material. From [3], Table 9-7, the lap-shear strength can be anywhere from $10.3 - 27.6MPa$. $10.3MPa$ will be selected as a conservative estimate.

The outer material is aluminium and the inner material will be carbon fibre. Because of the nature of aluminium, an extremely thin layer of fibreglass should be added between the carbon fibre and aluminium to prevent corrosion due to the curing of the epoxy. Data was found as follows:

$$\begin{aligned} G &= 1.3GPa \text{ [19]} \\ E_i &= 109GPa \text{ [14]} \\ \alpha_i &= 23.7 * 10^{-6}mm/mm^{\circ}C \text{ [14]} \\ E_0 &= 71GPa \text{ [3]} \\ \alpha_0 &= 23.94mm/mm^{\circ}C \text{ [3]} \end{aligned}$$

ΔT can be estimated by assuming the epoxy is cured at room temperature ($20^{\circ}C$) and that the lowest temperature the blimp will be used at is $-40^{\circ}C$. This yields $\Delta T = -60^{\circ}C$. The thickness of the adhesive will be estimated as $h = 0.5mm$. As preliminary estimates, $t_0 = 9.73mm$, $t_i = 9.73mm$, $l = 30mm$, and $b = 50.80mm$. The force P can be estimated using **SOME STUFF** $P = 100N$.

Substituting these values into Equation 3.2 yields

$$\omega = \sqrt{\frac{1300MPa}{0.5mm} \left(\frac{1}{71000MPa * 9.73mm} + \frac{2}{109000MPa * 9.73mm} \right)} = 0.0930946mm^{-1} \quad (3.3)$$

Followed by substitution into Equation 3.1:

$$\begin{aligned} \tau(x) &= \frac{100N * 0.0930946mm^{-1}}{4 * 50.80mm * \sinh(0.0930946mm^{-1} * 30mm/2)} \cosh(0.0930946mm^{-1} * x) + \\ &\left[\frac{100N * 0.0930946mm^{-1}}{4 * 50.80mm * \cosh(0.0930946mm^{-1} * 30mm/2)} \left(\frac{2 * 71000MPa * 9.73mm - 1300MPa * 9.73mm}{2 * 71000MPa * 9.73mm + 1300MPa * 9.73mm} \right) + \right. \\ &\left. \frac{(23.7 * 10^{-6}mm/mm^{\circ}C - 23.94 * 10^{-6}mm/mm^{\circ}C) * (-60^{\circ}C) * 0.0930946mm^{-1}}{\left(\frac{1}{71000MPa * 9.73mm} + \frac{2}{109000MPa * 9.73mm} \right) \cosh(0.0930946mm^{-1} * 30mm/2)} \right] \sinh(0.0930946mm^{-1} * x) \\ &= 0.02416MPa * \cosh(0.0930946mm^{-1} * x) + [0.02098MPa + 0.1871MPa] \sinh(0.0930946mm^{-1} * x) \end{aligned} \quad (3.4)$$

at $x = l/2 = 30mm/2$, the shear is at a maximum value. Therefore, the shear force is $\tau = 0.4464MPa$, Yielding a safety factor of $\eta = 10.3MPa/0.4464MPa = 23.0734$.

Bibliography

- [1] Actuonix Motion Devices. Miniature Linear Motion Series - L12, 2016. URL <https://s3.amazonaws.com/actuonix/Actuonix+L12+Datasheet.pdf>.
- [2] Steven A. Brandt and American Institute of Aeronautics and Astronautics. *Introduction to aeronautics : a design perspective*. American Institute of Aeronautics and Astronautics, 2004. ISBN 9781563477010.
- [3] Budynas and Nisbett. Shigley's Mechanical Engineering Design, Eighth Edition. *Analysis*, page 1059, 2006. ISSN 0717-6163. doi: 10.1007/s13398-014-0173-7.2.
- [4] Szabolcs Füzesi. Static Thrust Calculator - STRC, 2017. URL http://www.godolloairport.hu/calc/strc{_}eng/index.htm.
- [5] HobbyKing. Rhino 2250mAh 3S 11.1v 40C Lipoly Pack, . URL https://hobbyking.com/en{_}us/rhino-2250mah-3s-11-1v-40c-lipoly-pack.html?{_}{_}{_}store=en{_}us.
- [6] HobbyKing. TURNIGY Plush 10amp Speed Controller w/BEC, . URL https://hobbyking.com/en{_}us/turnigy-plush-10amp-9gram-speed-controller.html.
- [7] HobbyKing. Turnigy 20A BRUSHED ESC, . URL https://hobbyking.com/en{_}us/turnigy-20a-brushed-esc.html?{_}{_}{_}store=en{_}us.
- [8] HobbyKing. PixFalcon Micro PX4 Autopilot, . URL https://hobbyking.com/en{_}us/pixfalcon-micro-px4-autopilot.html.
- [9] HobbyKing. UBLOX Micro M8N GPS Compass Module (1pc), . URL https://hobbyking.com/en{_}us/ublox-micro-m8n-gps-compass-module-1pc.html.
- [10] HobbyKing. Aerostar Carbon Fibre Propeller 7x5, . URL https://hobbyking.com/en{_}us/aerostar-carbon-fibre-propeller-7x5-1pcs.html?{_}{_}{_}store=en{_}us.
- [11] HobbyKing. FrSky TFR6M 2.4Ghz 6CH Micro Receiver FASST Compatible, . URL https://hobbyking.com/en{_}us/frsky-tfr6m-2-4ghz-6ch-micro-receiver-fasst-compatible.html.
- [12] HobbyKing. HobbyKing® TM 2612 Brushless Outrunner 1900KV, . URL https://hobbyking.com/en{_}us/hobbykingr-tm-2612-brushless-outrunner-1900kv.html?gclid=CjwKCAjwgvf0BRB7EiwAeP7ehmx-1gQwKEcajtpPc1NNf0p82N1T2DdM6I-PF0INiIxTERGAN2ZBdhoCJIQQAvD{_}BwE{\&}gclsrc=aw.ds.
- [13] HobbyKing. Micro HKPilot Telemetry radio Set With Integrated PCB Antenna 915Mhz, . URL https://hobbyking.com/en{_}us/micro-hkpilot-telemetry-radio-set-with-integrated-pcb-antenna-915mhz.html.

- [14] MatWeb. Overview of materials for Epoxy/Carbon Fiber Composite, 2017. URL <http://www.matweb.com/search/DataSheet.aspx?MatGUID=39e40851fc164b6c9bda29d798bf3726{\&}ckck=1>.
- [15] McMaster-Carr. McMaster-Carr - Neoprene Roller, Drive, Aluminum Hub, 5/8" Roller Diameter, 3/16" Roller Width, . URL <https://www.mcmaster.com/{\#}60885k31/=19r8ni4>.
- [16] McMaster-Carr. McMaster-Carr - General Purpose Plastic Ball Bearing, with Stainless Steel Ball, for 1/4" Shaft Diameter, 5/8" OD, . URL <https://www.mcmaster.com/{\#}6455k2/=19nl4h4>.
- [17] McMaster-Carr. McMaster-Carr - Alloy Steel Cup-Point Set Screw, Black Oxide, 8-32 Thread, 1/4" Long, . URL <https://www.mcmaster.com/{\#}91375a190/=19r8q0o>.
- [18] McMaster-Carr. Music-Wire Steel Torsion Sring, . URL <https://www.mcmaster.com/{\#}9271k641/=19nl8gv>.
- [19] Michigan Technological University. Properties of Selecet Matrices, 2017. URL <http://wwwmse.mtu.edu/{}drjohn/my4150/props.html>.
- [20] Pololu. 50:1 Micro Metal Gearmotor HP 6V, . URL <https://www.pololu.com/product/998/specs>.
- [21] Pololu. Magnetic Encoder Pair Kit for Micro Metal Gearmotors, 12 CPR, 2.7-18V (HPCB compatible), . URL <https://www.pololu.com/product/3081/pictures>.
- [22] RobotShop. HS-7950TH Ultra Torque HV Coreless Titanium Gear Servo - RobotShop. URL http://www.robotshop.com/ca/en/hs-7950th-ultra-torque-coreless-titanium-gear-servo.html?gclid=CjwKCAjwgvf0BRB7EiwAeP7ehmVw7Ku4Ih2HYJeFV34wtpf0lmQIOCX5BXYQ00f48oI4lG0zHuABnRoCKiEQAvD{_}BwE.
- [23] Gabriel Staples. Propeller Static & Dynamic Thrust Calculation - Part 1 of 2, 2013. URL <http://www.electricrcaircraftguy.com/2013/09/propeller-static-dynamic-thrust-equation.html>.
- [24] Gabriel Staples. Propeller Static & Dynamic Thrust Calculation - Part 2 of 2, 2015. URL <http://www.electricrcaircraftguy.com/2014/04/propeller-static-dynamic-thrust-equation-background.html>.
- [25] Wikipedia. Cauchy Stress Tensor, 2017. URL https://en.wikipedia.org/wiki/Cauchy{_}stress{_}tensor.

Appendix A: Instructions for Installing and Running the GUI

yep

Appendix B: Code

B.1 Code 1

```
1 function lab1
2
3 disp('_____');
4 disp('_____');
5 disp('| Lab 1 |');
6 disp('_____');
7 disp('_____');
8
9
10 % Point we are using as x_i
11 x = 5.0;
12
13 % Delta x's that we will use in our finite-difference approximations
14 dx1 = 0.5;
15 dx2 = dx1/2;
16 dx3 = dx2/2;
17 dx4 = dx3/2;
18 dx5 = dx4/2;
19
20 % Exact derivative of y at x=5
21 exact1 = dy(5.0);
22
23 %%%%%%
24 % Approximation of the first derivative
25
26 approx11 = dyapprox(x, dx1);
27 approx12 = dyapprox(x, dx2);
28 approx13 = dyapprox(x, dx3);
29 approx14 = dyapprox(x, dx4);
30 approx15 = dyapprox(x, dx5);
31
32 % Errors using first-order method
33 disp('Errors for first-order finite-difference , (first column of table)')
34 error11 = abs(exact1 - approx11)
35 error12 = abs(exact1 - approx12)
36 error13 = abs(exact1 - approx13)
37 error14 = abs(exact1 - approx14)
38 error15 = abs(exact1 - approx15)
```

```

40 % Order of convergence
41 disp('Actual order of convergence for first-order method, (second column of table)')
42 order11 = log(error12/error11)/log(dx2/dx1)
43 order12 = log(error13/error12)/log(dx3/dx2)
44 order13 = log(error14/error13)/log(dx4/dx3)
45 order14 = log(error15/error14)/log(dx5/dx4)
46
47%%%%%%%%%%%%%
48 % Approximation of the second derivative
49
50 %Exact second derivative of y at x=5
51 exact2 = d2y(5.0);
52
53 approx21 = d2yapprox(x, dx1);
54 approx22 = d2yapprox(x, dx2);
55 approx23 = d2yapprox(x, dx3);
56 approx24 = d2yapprox(x, dx4);
57 approx25 = d2yapprox(x, dx5);
58
59 % Errors using first-order method
60 disp('Errors for first-order finite-difference, (first column of table)')
61 error21 = abs(exact2 -approx21)
62 error22 = abs(exact2 -approx22)
63 error23 = abs(exact2 -approx23)
64 error24 = abs(exact2 -approx24)
65 error25 = abs(exact2 -approx25)
66
67 % Order of convergence
68 disp('Actual order of convergence for first-order method, (second column of table)')
69 order21 = log(error22/error21)/log(dx2/dx1)
70 order22 = log(error23/error22)/log(dx3/dx2)
71 order23 = log(error24/error23)/log(dx4/dx3)
72 order24 = log(error25/error24)/log(dx5/dx4)
73
74%%%%%%%%%%%%%
75 % Approximation of the third derivative
76
77 %Exact third derivative of y at x=5
78 exact3 = d3y(5.0);
79
80 approx31 = d3yapprox(x, dx1);
81 approx32 = d3yapprox(x, dx2);
82 approx33 = d3yapprox(x, dx3);
83 approx34 = d3yapprox(x, dx4);
84 approx35 = d3yapprox(x, dx5);

```

```

85
86 % Errors using first-order method
87 disp('Errors for first-order finite-difference, (first column of table)')
88 error31 = abs(exact3 -approx31)
89 error32 = abs(exact3 -approx32)
90 error33 = abs(exact3 -approx33)
91 error34 = abs(exact3 -approx34)
92 error35 = abs(exact3 -approx35)
93
94 % Order of convergence
95 disp('Actual order of convergence for first-order method, (second column of table)')
96 order31 = log(error32/error31)/log(dx2/dx1)
97 order32 = log(error33/error32)/log(dx3/dx2)
98 order33 = log(error34/error33)/log(dx4/dx3)
99 order34 = log(error35/error34)/log(dx5/dx4)
100
101%%%%%%%%%%%%%
102%%%%%%%%%%%%%
103% Produce plots
104%%%%%%%%%%%%%
105%%%%%%%%%%%%%
106
107% Number of points in the plots
108% - Adjust this to adjust how small Delta x gets.
109% It starts at 1/2 and is divided by 2 "n" times
110 n = 33;
111
112% Initialize Storage
113 dxs = zeros(n,1);
114 errors1 = zeros(n,1);
115 errors2 = zeros(n,1);
116 errors3 = zeros(n,1);
117
118% loop through, filling "d_xs", "errors1", "errors2", and "errors3".
119 for i = 1:n
120 % Each time through the loop, Delta x is half as big
121 d_xs(i) = 0.5^i;
122 errors1(i)=abs(exact1-dyapprox(x,d_xs(i)));
123 errors2(i)=abs(exact2-d2yapprox(x,d_xs(i)));
124 errors3(i)=abs(exact3-d3yapprox(x,d_xs(i)));
125 end
126
127% Compute the log of the inverse of delta x
128 loginvdxs = log10(1./d_xs);
129

```

```

130 % Compute the log of the errors
131 logerrors1 = log10(errors1);
132 logerrors2 = log10(errors2);
133 logerrors3 = log10(errors3);
134
135 % Compute reference lines with the expected slope
136 %   - the "-2" is just an offset so that the reference
137 %     line does not intersect the error line.
138 refline1 = -3*loginvdxs -2;
139 refline2 = -2*loginvdxs -2;
140 refline3 = -1*loginvdxs -2;
141
142 %%%%%%
143 % Make three figures
144 figure(1);
145 plot(loginvdxs,logerrors1,'-o',loginvdxs,refline1)
146 legend('finite-difference','reference', 'slope = -3')
147 title('Third-order finite-difference error for the first derivative as a function of Delta x')
148 xlabel('log10(1/Delta x)')
149 ylabel('log10(error)')
150
151 figure(2);
152 plot(loginvdxs,logerrors2,'-o',loginvdxs,refline2)
153 legend('finite-difference','reference', 'slope = -2')
154 title('Second-order finite-difference error for the second derivative as a function of Delta x')
155 xlabel('log10(1/Delta x)')
156 ylabel('log10(error)')
157
158 figure(3);
159 plot(loginvdxs,logerrors3,'-o',loginvdxs,refline3)
160 legend('finite-difference','reference', 'slope = -1')
161 title('First-order finite-difference error for the third derivative as a function of Delta x')
162 xlabel('log10(1/Delta x)')
163 ylabel('log10(error)')
164
165 end
166
167
168 %%%%%%
169 % The function we are analysing evaluated at x
170 %%%%%%
171 function output = y(x)

```

```

172     output = (x^3)*sin(x);
173 end
174
175 %% The exact derivative of the function we are analysing
176 % evaluated at x.
177 %% evaluated at x.
178 %% evaluated at x.
179 function output = dy(x)
180     output = 3*x^2*sin(x)+x^3*cos(x);
181 end
182
183 %% The exact second derivative of the function we are analysing
184 % evaluated at x.
185 %% evaluated at x.
186 %% evaluated at x.
187 function output = d2y(x)
188     output = 6*x^2*cos(x)+(6*x-x^3)*sin(x);
189 end
190
191 %% The exact third derivative of the function we are analysing
192 % evaluated at x.
193 %% evaluated at x.
194 %% evaluated at x.
195 function output = d3y(x)
196     output = (18*x-x^3)*cos(x)+(6-9*x^2)*sin(x);
197 end
198
199 %% A third-order approximation to the derivative of y
200 % at x using a step size of "dx"
201 %% evaluated at x.
202 %% evaluated at x.
203 function output = dyapprox(x,dx)
204     output = (1.0/(6*dx))*(-11*y(x)+18*y(x+dx)-9*y(x+2*dx)+2*y(x+3*dx));
205 end
206
207 %% A second-order approximation to the second derivative of y
208 % at x using a step size of "dx"
209 %% evaluated at x.
210 %% evaluated at x.
211 function output = d2yapprox(x,dx)
212     output = 1.0/(dx*dx)*(2*y(x)-5*y(x+dx)+4*y(x+2*dx)-y(x+3*dx));
213 end
214
215 %% A first-order approximation to the third derivative of y
216 %% evaluated at x.

```

```
217 % at x using a step size of "dx"
218 %%%
219 function output = d3yapprox(x,dx)
220     output = 1.0/(dx*dx*dx)*(-1*y(x)+3*y(x+dx)-3*y(x+2*dx)+y(x+3*dx));
221 end
```

Appendix C: Additional Material

C.1 Thrust Force

Vectoring thrusters will be mounted to the both sides of the airship via the thruster supports attached to the keel. In order to encompass the forces that will be generated by the thruster, an equation will be used which was developed via research and experimental data collected and compiled by Gabriel Staples [24]. The basis of the equation is Newtons second law.

$$T = \frac{\partial(mv)}{\partial t} = \dot{m}v$$

based on this equation, in theory static thrust can be defined as

$$T_{static} = \dot{m}V_e$$

where V_e is the escape velocity of air through the thruster in m/s and \dot{m} is the mass flow of air through the thruster in kg/s . For dynamic thrust, which incorporates the movement of the airship,

$$T = \dot{m}\Delta V = \dot{m}(V_e - V_{as})$$

where V_{as} is the velocity of air coming into the thrusters in m/s but in a windless circumstance it is the airship velocity. Knowing that $\dot{m} = \rho A V_e$ and $A = \pi \frac{D^2}{4}$ where A is the area the propellers will cover in m^2 and D is the diameter of the propellers in m .

$$T = \rho \frac{\pi D^2}{4} (V_e^2 - V_e V_{as}) \quad (C.1)$$

There is obviously some proportionality between the escape velocity V_e and the tip velocity of the propeller. This claim can be supported by the fact that the tangential velocity of a propeller blade will be increasing along its radius, there for the greater the diameter the higher the tip speed. This velocity will affect the incident velocity of air it comes into contact with. Therefore a greater diameter will result in greater thrust as well as higher efficiency compared to a propeller of the same pitch with a lesser diameter [24]. This effect however tops out when the tip speed approaches the speed of sound. Pitch will also affect both the thrust and efficiency. Lower pitch diameter results in lower angle of attack. Lower angle of attack means less separation, less induced drag, as a result, higher diameter and lower pitch props will typically be more efficient [24].

In order to incorporate this into equation C.1, V_e is replaced with V_{pitch} which equals $RPM \cdot Pitch \cdot \frac{1min}{60s}$ where RPM is the rotations per minute of the motor, and $Pitch$ is the pitch diameter of the propeller blade in m . Equation C.1 is multiplied by a constant coefficient and the propeller diameter to pitch ratio to the power of a constant, as seen below in equation C.2.

$$T = \rho \frac{\pi D^2}{4} \left(K_1 \left(\frac{D}{Pitch} \right)^{K_2} \right) \left(\left(RPM \cdot Pitch \cdot \frac{1min}{60s} \right)^2 - V_{as} \left(RPM \cdot Pitch \cdot \frac{1min}{60s} \right) \right) \quad (\text{C.2})$$

The assumption that $V_e \approx V_{pitch}$ is not accurate. In addition, it is assumed that the air velocity across the area of the thruster will be constant, when in reality this is not the case [24]. Some of the error derived from these assumptions is corrected by the coefficient term in C.2. In order to choose these coefficients, a study done by Gabriel Staples [24] [23], compares data calculated with equation C.2 using varying constants, with experimental static thrust data from more than 150 tests which were done by multiple sources. These were used along with theoretical dynamic thrust data [2], and a smaller sample of experimental dynamic thrust data. The values for K_1 and K_2 that resulted in calculated thrust forces that best matched the experimental data were 0.16716 and 1.5. Since these values were determined using mainly static thrust data, they are more accurate when calculating static thrust. The highest forces will be generated during low speed or static thrusting so these will be the values used when modeling the parts supporting the thrusters. Results from comparing thrust values calculated using Gabriel Staples's equation C.3 and experimental data for both static and dynamic thrust can be found in appendix section C.1, Figures C.2 and C.3.

The following equation shows a sample calculation using an achievable motor RPM of 11000 from the HobbyKing 2612 Brushless Outrunner Motor 1900KV, whose specs can be seen in appendix section D.6.1. This RPM value was based off results obtained from an online calculator comparing required power values at varying RPMs to the power shown in appendix section C.1, Figures C.4. An airship speed of 10m/s was used.

$$T = \rho \frac{\pi D^2}{4} \left(0.16716 \left(\frac{D}{Pitch} \right)^{1.5} \right) \left(\left(RPM \cdot Pitch \cdot \frac{1min}{60s} \right)^2 - V_{as} \left(RPM \cdot Pitch \cdot \frac{1min}{60s} \right) \right) \quad (\text{C.3})$$

$$\begin{aligned} &= 1.225[\text{kg/m}^3] \frac{\pi(0.1778[\text{m}])^2}{4} \left(0.16716 \left(\frac{0.1778[\text{m}]}{0.127[\text{m}]} \right)^{1.5} \right) \left(\left(11000[\text{rpm}] \cdot 0.127[\text{m}] \cdot \frac{1min}{60s} \right)^2 \right. \\ &\quad \left. - 10[\text{m/s}] \left(11000[\text{rpm}] \cdot Pitch \cdot \frac{1min}{60s} \right) \right) = 2.604[\text{N}] \end{aligned}$$

Appendix section C.1, Figure C.1 depicts the decrease in thrust force with increasing airship speed. This phenomena can also be observed below in table C.1. At an RPM of 11000 as the air ship reaches

24m/s the thrust force goes to 0 indicating that this would be the maximum speed. Obviously there are several considerable forces such as gravitational forces, drag, and other aerodynamic forces which are not accounted and this is therefore not an accurate method of determining maximum speed.

Table C.1: Table of Calculated Thrust Values for Varying Airship Speeds

Airship Speed, V_{as} , (m/s)	Airship Speed, V_{as} (mph)	Thrust, T (N)	Thrust, T (g)	Thrust, T (kg)
0	0.000	4.566	465.403	0.465
1	2.237	4.370	445.414	0.445
2	4.474	4.173	425.425	0.425
3	6.711	3.977	405.436	0.405
4	8.948	3.781	385.448	0.385
5	11.185	3.585	365.459	0.365
6	13.422	3.389	345.470	0.345
7	15.659	3.193	325.482	0.325
8	17.896	2.997	305.493	0.305
9	20.132	2.801	285.504	0.286
10	22.369	2.605	265.516	0.266
11	24.606	2.409	245.527	0.246
12	26.843	2.213	225.538	0.226
13	29.080	2.016	205.550	0.206
14	31.317	1.820	185.561	0.186
15	33.554	1.624	165.572	0.166
16	35.791	1.428	145.584	0.146
17	38.028	1.232	125.595	0.126
18	40.265	1.036	105.606	0.106
19	42.502	0.840	85.617	0.086
20	44.739	0.644	65.629	0.066
21	46.976	0.448	45.640	0.046
22	49.213	0.252	25.651	0.026
23	51.450	0.056	5.663	0.006
24	53.687	-0.141	-14.326	-0.014

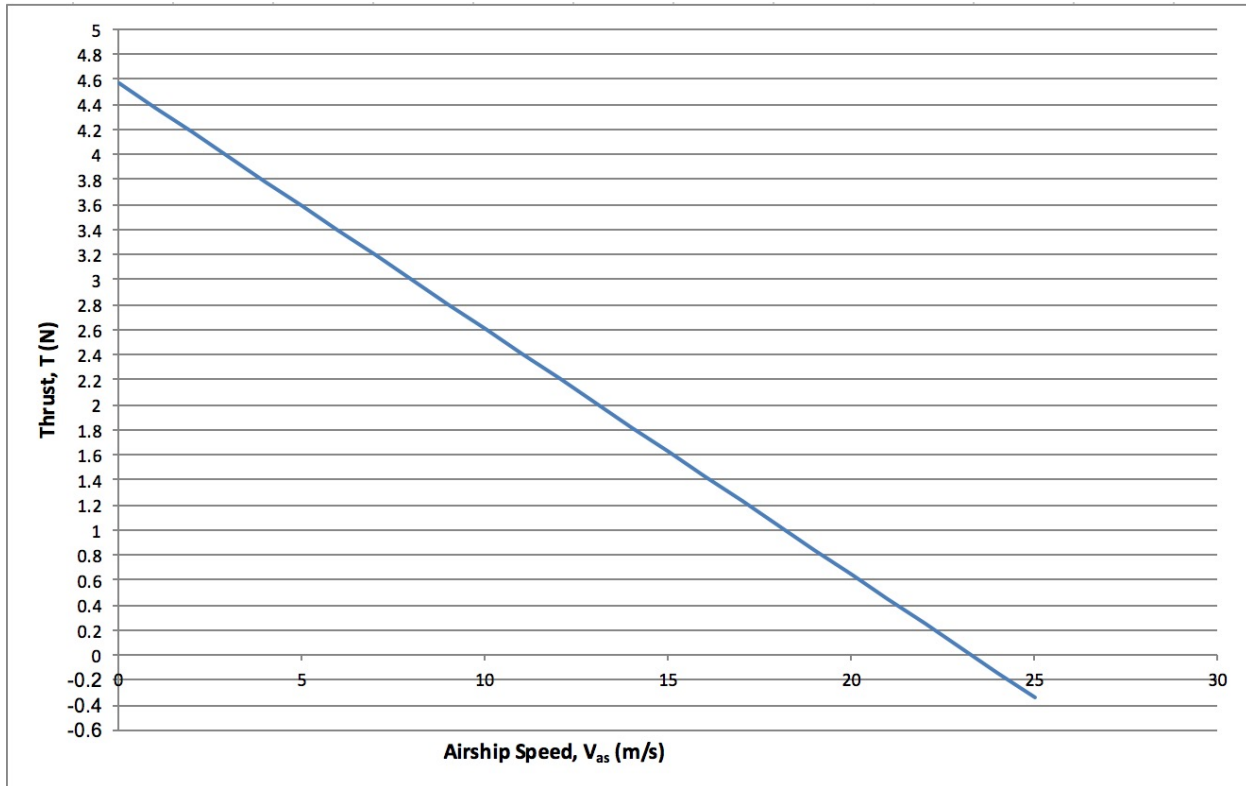


Figure C.1: Graph of Thrust Plotted Against Airship Speed at 11000rpm With 7", 5" Pitch Diameter Propeller

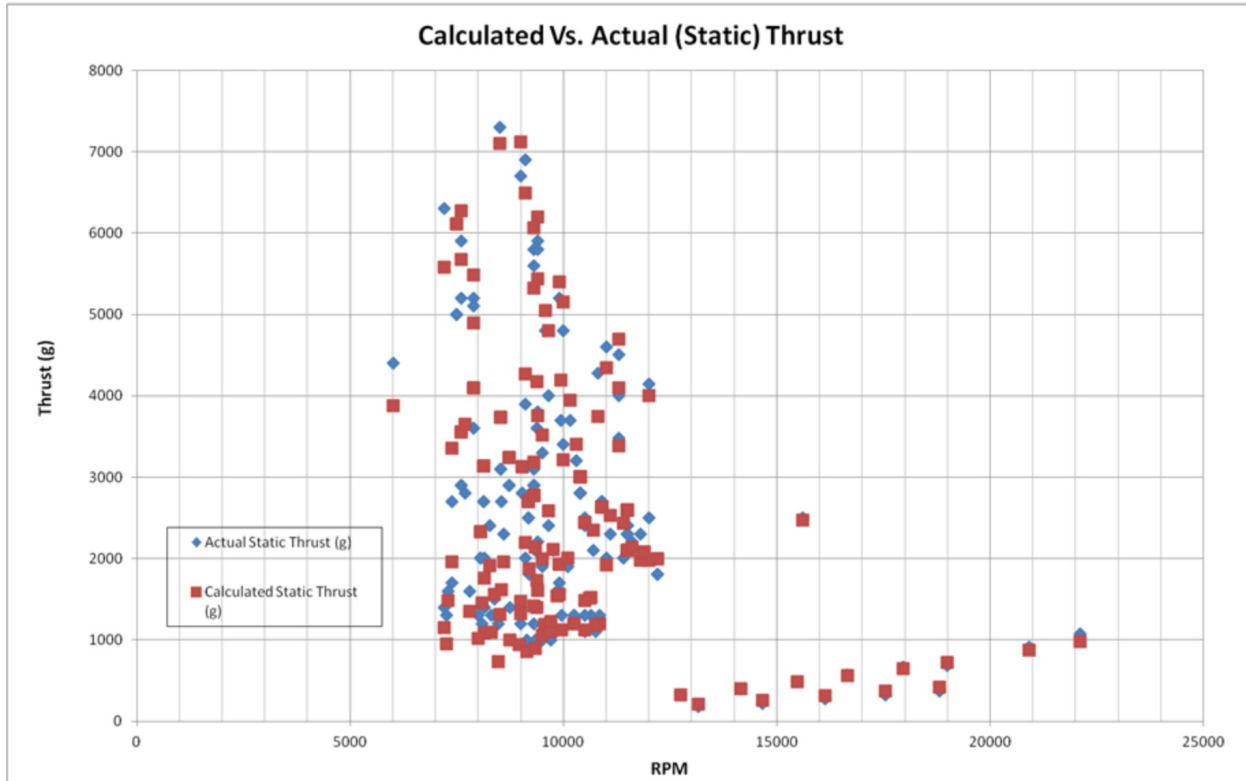


Figure C.2: Test Data from Gabriel Staples Against Experimental Static Thrust Values [24]

Propeller Dynamic Thrust - Experimental Results vs. Semi-empirical Calculation

10x6 propeller, Full Throttle

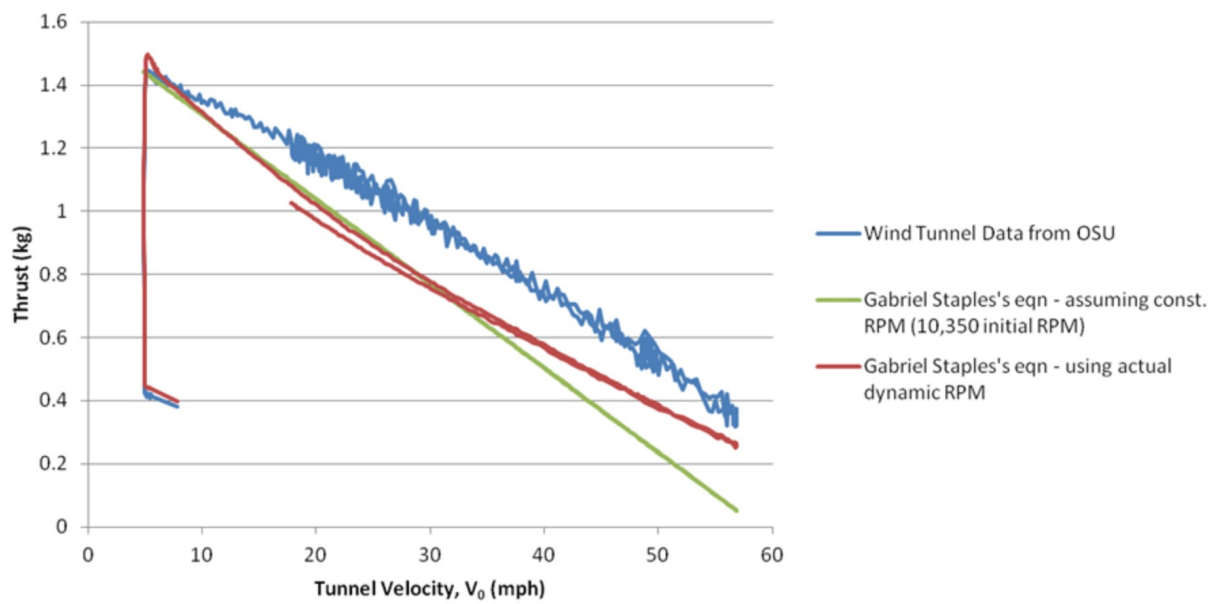


Figure C.3: Test Data from Gabriel Staples Against Experimental Dynamic Thrust Values [24]

Propeller diameter	7	inch
Pitch	5	inch
Propeller type	Standard propeller	
	CF	1
No. of blades	2	<input type="button" value="▼"/>
RPM	11000	
Air temperature	68 Fahrenheit	
Air density	1.2045 (kg/m ³)	
Static thrust = 12.34 oz		
Static thrust = 0.79 pound		
Static thrust = 0.35 kg		
Perimeter speed = 102.35 m/s		
Required engine power = 0.108 HP = 0.079 kW		
Estimated flying speed = 52.0 mph = 45.1 Knots		

Figure C.4: Sample Thrust Calculation Using On-line Calculator [4]

C.2 Cauchy Stress Tensor [25]

The Cauchy Stress tensor fully defines the stresses acting on an infinitesimally small element within a material. It is particularly useful for failure analysis, as it is the internal stresses within a material that are used to determine the safety factor of the material at a specific location. Its general forms are shown below.

$$\sigma = \begin{bmatrix} \sigma_{11} & \sigma_{12} & \sigma_{13} \\ \sigma_{21} & \sigma_{22} & \sigma_{23} \\ \sigma_{31} & \sigma_{32} & \sigma_{33} \end{bmatrix} \equiv \begin{bmatrix} \sigma_{xx} & \sigma_{xy} & \sigma_{xz} \\ \sigma_{yx} & \sigma_{yy} & \sigma_{yz} \\ \sigma_{zx} & \sigma_{zy} & \sigma_{zz} \end{bmatrix} \equiv \begin{bmatrix} \sigma_x & \tau_{xy} & \tau_{xz} \\ \tau_{yx} & \sigma_y & \tau_{yz} \\ \tau_{zx} & \tau_{zy} & \sigma_z \end{bmatrix} \quad (\text{C.4})$$

Generally, the use of failure theories requires knowing the *principal stresses*. These are located perpendicular to the *principal planes*. Any body in a state of stress will have three principal planes, where there are no normal shear stresses, only three *principal stresses*.

Any stress tensor can undergo a change of coordinates to obtain the principal stresses. The transformed stress tensor can be written as follows:

$$\sigma' = \begin{bmatrix} \sigma_1 & 0 & 0 \\ 0 & \sigma_2 & 0 \\ 0 & 0 & \sigma_3 \end{bmatrix} \quad (\text{C.5})$$

Obtaining the principle stresses is relatively simple. The principle stresses are simply the eigenvalues of the stress tensor. MATLAB is used to find the eigenvalues of a given stress tensor, and the principle stresses are given by

$$\sigma_1 = \max(\lambda_1, \lambda_2, \lambda_3) \quad (\text{C.6})$$

$$\sigma_3 = \min(\lambda_1, \lambda_2, \lambda_3) \quad (\text{C.7})$$

$$\sigma_2 = \sigma_{11} + \sigma_{22} + \sigma_{33} - \sigma_1 - \sigma_3 \quad (\text{C.8})$$

The principal stresses are then used to conduct failure analysis using the preferred failure analysis method (e.g. Von Mises).

Appendix D: Data Sheets

D.1 Linear Actuator [1]



100mm L12 Actuator
Actual Size

Benefits

- Compact
- Simple control
- Low voltage
- Equal push/pull
- Easy mounting

Applications

- Robotics
- Appliances
- Toys
- RC vehicles
- Automotive
- Industrial Automation

Miniature Linear Motion Series · L12

Actuonix Motion Devices unique line of Miniature Linear Actuators enables a new generation of motion-enabled product designs, with capabilities that have never before been combined in a device of this size. These small linear actuators are a superior alternative to designing with awkward gears, motors, servos, and linkages.

Actuonix's L series of micro linear actuators combine the best features of our existing micro actuator families into a highly flexible, configurable, and compact platform with an optional sophisticated on-board microcontroller. The first member of the L series, the L12, is an axial design with a powerful drive-train and a rectangular cross section for increased rigidity. But by far the most attractive feature of this actuator is the broad spectrum of available configurations.

L12 Specifications

Gearing Option	50:1	100:1	210:1
Peak Power Point	17N @ 14mm/s	31N @ 7mm/s	62N @ 3.2mm/s
Peak Efficiency Point	10N @ 19mm/s	17N @ 10mm/s	36N @ 4.5mm/s
Max Speed (<i>no load</i>)	25mm/s	13mm/s	6.5mm/s
Max Force (<i>lifted</i>)	22N	42N	80N
Back Drive Force (<i>static</i>)	12N	22N	45N
Stroke Option	10 mm	30mm	50mm
Mass	28 g	34 g	40 g
Repeatability (-I, -R, -P&LAC)	±0.1 mm	±0.2 mm	±0.3 mm
Max Side Load (<i>extended</i>)	50N	40N	30N
Closed Length (<i>hole to hole</i>)	62mm	82mm	102mm
Potentiometer (-I, -R, -P)	1kΩ±50%	3kΩ±50%	6kΩ±50%
Voltage Option	6VDC	12VDC	
Max Input Voltage	7.5V	13.5V	
Stall Current	460mA	185mA	
Standby Current (-I/-R)	7.2mA	3.3mA	
Operating Temperature	-10°C to +50°C		
Potentiometer Linearity	Less than 2.00%		
Max Duty Cycle	20 %		
Audible Noise	55dB @ 45cm		
Ingress Protection	IP-54		
Mechanical Backlash	0.2mm		
Limit Switches (-S)	Max. Current Leakage: 8uA		
Maximum Static Force	200N		

1 - Control Option Specific values are identified with -I, -R, -P, -S, and LAC

2 - 1 N (Newton) = 0.225 lbf (pound-force) & 25.4mm=1 Inch

3 - A powered-off actuator will statically hold a force up to the Backdrive Force

4 - Actuators should be tested in each specific application to determine their effective life under those loading conditions and environment.

All information provided on this datasheet is subject to change. Purchase or use of Actuonix actuators is subject to acceptance of our terms and conditions as posted here: <http://www.actuonix.com/terms.asp>



Actuonix Motion Devices Inc

580 Starling Lane

Victoria, BC, V9E 2A9

Canada

1(206) 347-9684 phone

1(888) 225-9198 toll-free

1(206) 347-9684 fax

sales@actuonix.com

Copyright 2016 © Actuonix Motion Devices Inc.

D.2 Bearings [16]

10/10/2017

McMaster-Carr - General Purpose Plastic Ball Bearing, with Stainless Steel Ball, for 1/4" Shaft Diameter, 5/8" OD



General Purpose Plastic Ball Bearing with Stainless Steel Ball, for 1/4" Shaft Diameter, 5/8" OD

In stock
\$6.03 Each
6455K2



Bearing Type	Ball
For Load Direction	Radial
Ball Bearing Type	Standard
Construction	Single Row
Seal Type	Open
For Shaft Shape	Round
Trade No.	R4
For Shaft Diameter	1/4"
ID	0.25"
ID Tolerance	0" to 0.003"
OD	5/8"
OD Tolerance	-0.003" to 0"
Width	0.196"
Width Tolerance	-0.005" to 0.005"
Material	Acetal
Cage Material	Plastic
Radial Load Capacity, lbs.	
Dynamic	25
Static	15
Maximum Speed	2,300 rpm
Shaft Mount Type	Press Fit
Lubrication	Not Required
Temperature Range	-40° to 180° F
ABEC Rating	Not Rated
Radial Clearance	0.001" to 0.008"
Ball Material	Stainless Steel
RoHS	Compliant

Choose these acetal bearings for their all-around corrosion and chemical resistance.

Stainless steel balls offer excellent corrosion resistance.

D.3 Friction Wheel Assembly

D.3.1 Friction Wheel [15]

10/10/2017

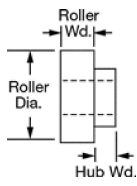
McMaster-Carr - Neoprene Roller, Drive, Aluminum Hub, 5/8" Roller Diameter, 3/16" Roller Width



Neoprene Roller

Drive, Aluminum Hub, 5/8" Roller Diameter, 3/16" Roller Width

In stock
\$16.70 Each
60885K31



Guide Roller Type	Drive
Roller Style	Shaft Mount
Roller Profile	Flat
Roller Material	Neoprene
Hub Material	Aluminum
Roller	
Diameter	5/8"
Width	3/16"
For Shaft Diameter	1/4"
Hub	
Diameter	1/2"
Width	1/4"
Shaft Mount Type	Set Screw
Set Screws	
Number Required	1
Included	No
Thread Size	8-32
Temperature Range	-40° to 170° F
Durometer (Hardness Rating)	55A (Medium) Black
RoHS	Compliant
Related Product	8-32 Stainless Steel Cup Point Set Screws (100/Pkg.)

Made of neoprene rubber, these rollers resist oil, flames, gasoline, and weather. Also known as contact wheels and feed rollers, they have tapped hubs that allow you to mount them onto a shaft or stud to transmit power.

D.3.2 Friction Wheel Set Screw [17]

10/10/2017

McMaster-Carr - Alloy Steel Cup-Point Set Screw, Black Oxide, 8-32 Thread, 1/4" Long



Alloy Steel Cup-Point Set Screw
Black Oxide, 8-32 Thread, 1/4" Long

In stock
\$10.65 per pack of 100
91375A190



Material	Black-Oxide Alloy Steel
Thread Size	8-32
Length	1/4"
Drive Size	5/64"
Screw Size Decimal Equivalent	0.164"
Hardness	Rockwell C45
Specifications Met	ASME B18.3, ASTM F912
Thread Type	UNC
Thread Spacing	Coarse
Thread Fit	Class 3A
Thread Direction	Right Hand
Drive Style	Hex
Tip Type	Cup
Head Type	Headless
System of Measurement	Inch
RoHS	Compliant

Made from alloy steel, these set screws have a thin edge that digs into hard surfaces for a secure hold. Length listed is the overall length.

Black-oxide alloy steel set screws resist corrosion in dry environments.

D.3.3 Friction Wheel Motor [20]

10/10/2017

Pololu - 50:1 Micro Metal Gearmotor HP 6V

50:1 Micro Metal Gearmotor HP 6V



www.pololu.com

Pololu item #: 998 438 in stock

Price break	Unit price (US\$)
1	15.95
10	13.55
50	11.96

Quantity: Add to cart[backorders allowed](#) Add to wish list

This gearmotor is a miniature **high-power, 6 V** brushed DC motor with a **51.45:1** metal gearbox. It has a cross section of 10 × 12 mm, and the D-shaped gearbox output shaft is 9 mm long and 3 mm in diameter.

Key specs at 6 V: 625 RPM and 120 mA with no load, 15 oz-in (1.1 kg-cm) and 1.6 A at stall.

Select options:

[Description](#) [Specs \(10\)](#) [Pictures \(20\)](#) [Resources \(12\)](#) [FAQs \(1\)](#) [On the blog \(1\)](#)

Dimensions

Size:	10 × 12 × 26 mm ¹
Weight:	9.5 g
Shaft diameter:	3 mm ²

General specifications

Gear ratio:	51.45:1
Free-run speed @ 6V:	630 rpm
Free-run current @ 6V:	120 mA
Stall current @ 6V:	1600 mA
Stall torque @ 6V:	15 oz·in
Extended motor shaft?:	N

<https://www.pololu.com/product/998/specs>

1/2

D.3.4 Friction Wheel Encoder [21]

10/10/2017

Pololu - Magnetic Encoder Pair Kit for Micro Metal Gearmotors, 12 CPR, 2.7-18V (HPCB compatible)

Magnetic Encoder Pair Kit for Micro Metal Gearmotors, 12 CPR, 2.7-18V (HPCB compatible)

Pololu item #: 3081 **574** in stock

Price break	Unit price (US\$)
1	8.95
10	7.95
50	6.95

Quantity: **Add to cart**

backorders allowed **Add to wish list**

Navigation icons: back, forward, first, last.

Add quadrature encoders to your micro metal gearmotors (extended back shaft version required) with this kit that uses a magnetic disc and hall effect sensors to provide 12 counts per revolution of the motor shaft. The sensors operate from 2.7 V to 18 V and provide digital outputs that can be connected directly to a microcontroller or other digital circuit. This module is compatible with **all** of the dual-shaft micro metal gearmotors we carry, including the HPCB versions.

[Description](#) [Specs \(6\)](#) [Pictures \(13\)](#) [Resources \(5\)](#) [FAQs \(0\)](#) [On the blog \(4\)](#)

Overview

This kit includes two dual-channel Hall Effect sensor boards and two **6-pole magnetic discs** that can be used to add quadrature encoding to two **micro metal gearmotors with extended back shafts** (motors are not included with this kit). The encoder board senses the rotation of the magnetic disc and provides a resolution of 12 counts per revolution of the motor shaft when counting both edges of both channels. To compute the counts per revolution of the gearbox output shaft, multiply the gear ratio by 12.

D.4 Spring [18]

10/10/2017

McMaster-Carr - Music-Wire Steel Torsion Spring, 180 Degree Right-Hand Wound, 0.767" OD



Music-Wire Steel Torsion Spring 180 Degree Right-Hand Wound, 0.767" OD

In stock
\$8.06 per pack of 6
9271K271



Spring Type	Torsion
Material	Music-Wire Steel
Deflection Angle	180°
Wind Direction	Right Hand
OD	0.767"
For Maximum Shaft Diameter	0.500"
Wire Diameter	0.063"
Leg Length	2,000"
Number of Coils	6.00
Spring Length @ Maximum Torque	0.475"
Maximum Torque	5,518 in.-lbs.
RoHS	Compliant

These music-wire steel springs are stronger than stainless steel springs. Commonly found in clothespins, spring clamps, mousetraps, motors, and spring-return mechanisms, torsion springs maintain pressure over a short distance in a rotational direction. They are often supported by a shaft, mandrel, or arbor.

Squeezing a torsion spring reduces its OD, which tightens the spring around a shaft and increases the spring length. Since the spring gets tighter as it is squeezed around the shaft, a maximum shaft diameter for each spring is listed. Using a shaft with a larger diameter will interfere with the spring motion.

Torsion springs should be used in the direction in which the coils are wound. Deflection angle represents the angle between the legs of the spring as well as the maximum spring rotation. All springs rotate until their legs are parallel. For example, a spring with a 90° deflection angle has a 90° angle between its legs, and it will rotate a maximum of 90°. Maximum torque is the torque required to rotate the spring legs to the parallel position.

D.5 Battery [5]

Rhino 2250mAh 3S 11.1v 40C Lipoly Pack



Specifications

SKU:	R2250-40-3	Brand:	N/A
Weight(g)	243.00	Length	109.00
Width:	26.00	Height:	36.00
Capacity (mAh)	2250.00	Discharge(c)	40.00
Length-A(mm):	107.00	Height-B(mm):	34.00
Width-C(mm)	26.00	Unit Weight (g)	191
Max Charge Rate(C):	5.00	Discharge Plug:	N/A

D.6 Thruster Assembly

D.6.1 Thruster Motor [12]

HobbyKing®™ 2612 Brushless Outrunner 1900KV



Specifications

RPM/V: **1900Kv**
Cell Count: **2~3s Lipoly**
Max.efficiency: **78.0%**
Current at Max.eff: **6.3~8.7A**
Max.current: **14A**
No Load Current: **0.8A/7V**
Internal Resistance: **165mOhm**
Diameter: **27mm**
Length: **23.4mm**
Mounting Hole Spacings: **32mm**
Mounting Hole Diameter: **2mm**
Shaft: **3mm**
Weight: **25g**

D.6.2 Propeller [10]

Aerostar Carbon Fibre Propeller 7x5



Specifications

SKU:	9445000180-0	Brand:	N/A
Weight(g)	14.00	Length	180.00
Width:	15.00	Height:	20.00
Pitch Y(inch)	5.00	Material	Carbon Fiber
Rotation:	CCW	Unit Weight (g):	N/A
Type	Normal	Blade Count	2
Diameter X(inch):	7.00		

D.6.3 BEC [6]

TURNIGY Plush 10amp Speed Controller w/BEC



Specifications

Cont Current: 10A	SKU:	TR_P10A
Burst Current: 12A	Weight(g)	20.00
BEC Mode: Linear	Width:	10.00
BEC : 5v / 2A	Brand:	No
Lipo Cells: 2-4	Length	110.00
NiMH : 5-12	Height:	110.00
Weight: 9g		
Size: 27x17x6mm		

D.6.4 Servo Motor [22]

RB-Hit-128

HS-7950TH Ultra Torque HV Coreless Titanium Gear Servo



Hitec's strongest servo period, the "Ultra Torque" HS-7950TH is designed to operate on a two cell LiPo Pack. Featuring our high resolution "G2" second generation programmable digital circuit and our indestructible Titanium gears, the HS-7950TH has the performance and durability you've come to expect from a Hitec servo. Other features in the HS-7950TH include a 7.4V optimized coreless motor, integrated heat sink case, and a top case with two hardened steel gear pins supported by axial brass bushing.

The HS-7950TH has been designed for the most demanding hobby applications including the largest aircraft and monster trucks. Featuring a titanic 403 oz./in. of torque at 6.0 volts, while still maintaining a respectable 0.15 second transit time.

Features

- G2 Digital Circuit
- Titanium Gear Train (MK first gear)

- Ultra Performance Coreless Motor
- Heatsink Case
- (8) O-Rings for Water/Dust/Fuel protection
- Dual Ball Bearing Supported Output Shaft

Programmable Features Include:

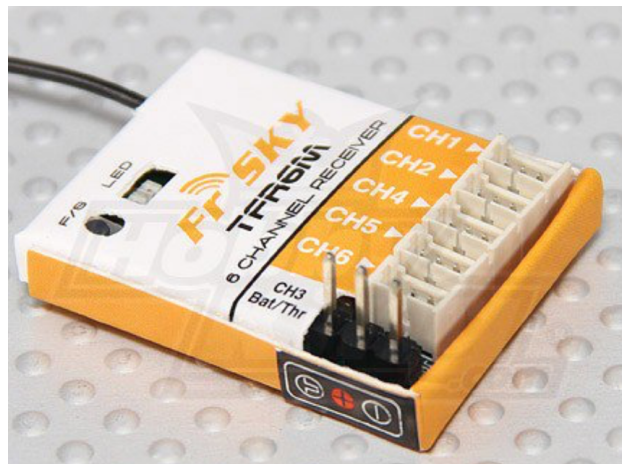
- Dead Band Width
- Direction of Rotation
- Speed of Rotation (slower)
- End Points
- Neutral Points
- Fail Safe On/Off
- Fail Safe Point
- Resolution* (default is high resolution)
- Overload Protection* (default is off)

Specifications

- Motor Type: Coreless
- Bearing Type: Dual Ball Bearing
- Speed (6.0V/7.4V): 0.15 / 0.13
- Torque oz./in. (6.0V/7.4V): 403 / 486
- Torque kg./cm. (6.0V/7.4V): 29.0 / 35.0
- Size in Inches: 1.57 x 0.79 x 1.50
- Size in Millimeters: 39.88 x 20.07 x 38.10
- Weight oz.: 2.40
- Weight g.: 68.04

D.6.5 Receiver [11]

FrSky TFR6M 2.4Ghz 6CH Micro Receiver FASST Compatible



Specification

SKU:	236000003	Brand:	FrSky
Weight(g)	34.00	Length	160.00
Width:	20.00	Height:	87.00

D.7 Flight Control Assembly

D.7.1 ESC [7]

Turnigy 20A BRUSHED ESC



Specifications

SKU:	TGY-20A	Brand:	No
Weight(g)	39.00	Length	150.00
Width:	10.00	Height:	110.00

D.7.2 GPS Module [9]

UBLOX Micro M8N GPS Compass Module

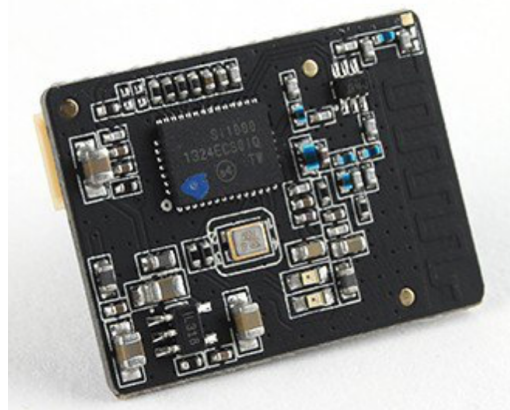


Specifications

SKU:	9387000083-0	Brand:	No
Weight(g)	29.00	Length	80.00
Width:	10.00	Height:	60.00

D.7.3 Transceiver [13]

Micro HKPilot Telemetry Radio Set with Integrated PCB
Antenna 915Mhz



Specifications

Supply voltage: **3.7-6 VDC**

Transmit current: **100 mA at 20 dBm**

Receive current: **25 mA**

Serial interface: **3.3 V UART**

Size: **19x25x5mm (with antenna)**

Weight: **1.6g (with antenna)**

Specs Ground Transceiver:

Supply voltage: **3.7-6 VDC (from USB or DF13 connector)**

Transmit current: **100 mA at 20 dBm**

Receive current: **25 mA**

Serial interface: **3.3 V UART**

Size: **25.5x 53x11 mm (without antenna)**

Weight: **11.5g (without antenna)**

SKU:	387000067-0	Brand:	No
Weight(g)	44.00	Length	100.00
Width:	40.00	Height:	70.00

D.7.4 Flight Controller [8]

PixFalcon Micro PX4 Autopilot



Specifications

SKU:	9387000082-0	Brand:	N/A
Weight(g)	99.00	Length	107.00
Width:	40.00	Height:	74.00

Appendix E: Engineering Drawings

E.1 Parts List

E.2 Complete System Drawing

including cross sections

E.3 Sub-Assembly Drawings

E.4 Individual Part Drawings

Appendix F: Meeting Minutes

Minutes

Appendix G: Recommendations for Improving the Course

lol